Hydrogen Storage Based on Physisorption

ARTICLE *in* THE JOURNAL OF PHYSICAL CHEMISTRY B · MAY 2009

Impact Factor: 3.3 · DOI: 10.1021/jp809097v · Source: PubMed

Hydrogen Storage Based on Physisorption

L. G. Scanlon,*,† W. A. Feld,‡ P. B. Balbuena,§ G. Sandi,⊥ X. Duan,# K. A. Underwood,‡ N. Hunter,‡ J. Mack,¶ M. A. Rottmayer,† and M. Tsao†

Air Force Research Laboratory, Electrochemistry & Thermal Sciences Branch, Wright-Patterson AFB, Ohio 45433, Department of Chemistry, Wright State University, Dayton, Ohio 45435, Department of Chemical Engineering, Texas A&M University, College Station, Texas 77843, Chemistry Division, Argonne National Laboratory, 9700 South Cass Avenue, Argonne, Illinois 60439, Air Force Research Laboratory, Major Shared Resource Center, Wright-Patterson AFB, Ohio 45433, and Department of Chemistry, University of Cincinnati, P.O. Box 210172, Cincinnati, Ohio 45221

Received: October 14, 2008; Revised Manuscript Received: January 17, 2009

Physisorption of molecular hydrogen based on neutral and negatively charged aromatic molecular systems has been evaluated using ab initio calculations to estimate the binding energy, ΔH, and ΔG at 298 (~77 bar) and 77 K (45 bar) in order to compare calculated results with experimental measurements of hydrogen adsorption. The molecular systems used in this study were corannulene ($C_{20}H_{10}$), dicyclopenta[*def*,*jkl*]triphenylene ($C_{20}H_{10}$), 5,8-dioxo-5,8-dihydroindeno[2,1-*c*]fluorene ($C_{20}H_{10}O_2$), 6-hexyl-5,8-dioxo-5,8-dihydroindeno[2,1-*c*]fluorene ($C_{26}H_{22}O_2$), coronene ($C_{24}H_{12}$), dilithium phthalocyanine (Li_2Pc, $C_{32}H_{16}Li_2N_8$), tetrabutylammonium lithium phthalocyanine (TBA-LiPc, $C_{48}H_{52}LiN_9$), and tetramethylammonium lithium phthalocyanine (TMA-LiPc, $C_{36}H_{28}LiN_9$). It was found (a) that the calculated term that corrects 0 K electronic energies to give Gibbs energies (thermal correction to Gibbs energy, TCGE) serves as a good approximation of the adsorbent binding energy required in order for a physisorption process to be thermodynamically allowed and (b) that the binding energy for neutral aromatic molecules varies as a function of curvature (e.g., corannulene versus coronene) or if electron-withdrawing or -donating groups are part of the adsorbent. A negatively charged aromatic ring, the lithium phthalocyanine complex anion, $[LiPc]^-$, introduces charge-induced dipole interactions into the adsorption process, resulting in a doubling of the binding energy of Li_2Pc relative to corannulene. Experimental hydrogen adsorption results for Li_2Pc, which are consistent with MD simulation results using χ-Li_2Pc to simulate the adsorbent, suggest that only one side of the phthalocyanine ring is used in the adsorption process. The introduction of a tetrabutylammonium cation as a replacement for one lithium ion in Li_2Pc has the effect of increasing the number of hydrogen molecules adsorbed from 10 (3.80 wt %) for Li_2Pc to 24 (5.93 wt %) at 77 K and 45 bar, suggesting that both sides of the phthalocyanine ring are available for hydrogen adsorption. MD simulations of layered tetramethylammonium lithium phthalocyanine molecular systems illustrate that doubling the wt % H_2 adsorbed is possible via such a system. Ab initio calculations also suggest that layered or sandwich structures can result in significant reductions in the pressure required for hydrogen adsorption.

1. Introduction

Physisorption is an attractive method for storing molecular hydrogen because a low enthalpy of adsorption/desorption makes hydrogen more readily accessible at ambient conditions when compared to chemisorption, in which temperatures on the order of 600 K are typically required for desorption. It has been suggested that in order to maximize the amount of adsorbed hydrogen accessible at 298 K and 1.5−30 bar, the enthalpy of adsorption should be in the range of −3.61 kcal/mol.[1] Activated carbons have been reported to have an enthalpy of adsorption on the order of −1.43 kcal/mol at 298 K, with binding energies on the order of −2.15 kcal/mol.[2,3] In addition, it has been suggested that binding energies of −4.78 to −9.56 kcal/mol are possible with small cations or anions[4] and that transition-metal-doped carbons or metal organic framework materials can be used to take advantage of the increased binding energy associated with the transition metal.[5] A binding energy of −6.93 kcal/mol has been predicted for hydrogen storage in organometallic buckyballs. The research reported herein focuses on a comparison of the calculated and experimental hydrogen adsorption properties of the aromatic phthalocyanine dianion (Pc^{2-}) with those of the neutral aromatics corannulene, coronene, and related compounds, with a particular emphasis on structural features that lead to enhanced adsorption at temperatures near 298 K and pressures under 100 bar.

2. Experimental Section

2.1. Materials. The molecular systems used in this study were corannulene ($C_{20}H_{10}$), dicyclopenta[*def*,*jkl*]triphenylene (isocoranulene, $C_{20}H_{10}$), 5,8-dioxo-5,8-dihydroindeno[2,1-*c*]fluorene (diketone, $C_{20}H_{10}O_2$), 6-hexyl-5,8-dioxo-5,8-dihydroindeno[2,1-*c*]fluorene (hexyldiketone, $C_{26}H_{22}O_2$), coronene ($C_{24}H_{12}$), dilithium phthalocyanine (Li_2Pc, $C_{32}H_{16}Li_2N_8$), tetrabutylammonium lithium phthalocyanine (TBA-LiPc,

* To whom correspondence should be addressed. E-mail: lawrence.scanlon@wpafb.af.mil.
† Electrochemistry & Thermal Sciences Branch, Wright-Patterson AFB.
‡ Wright State University.
§ Texas A&M University.
⊥ Argonne National Laboratory.
Major Shared Resource Center, Wright-Patterson AFB.
¶ University of Cincinnati.

10.1021/jp809097v CCC: $40.75
Published on Web 03/10/2009

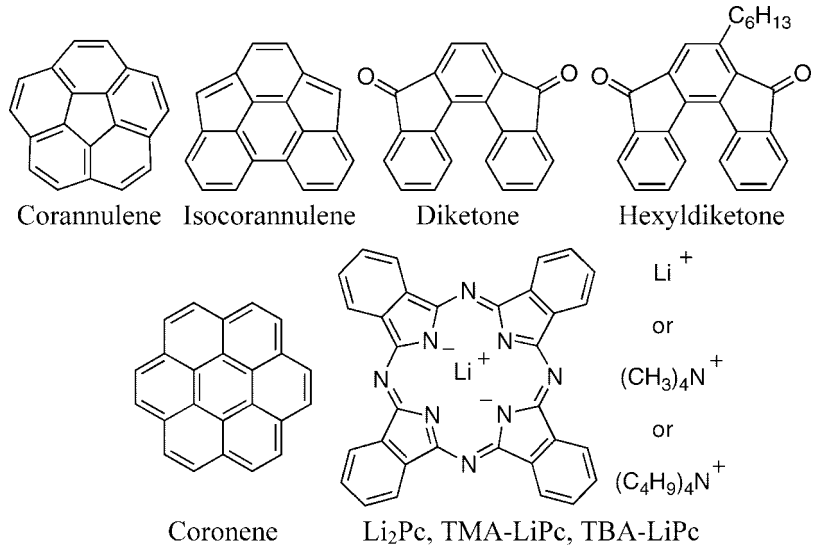

$C_{48}H_{52}LiN_9$), and tetramethylammonium lithium phthalocyanine (TMA-LiPc, $C_{36}H_{28}LiN_9$).

The synthesis of corannulene, diketone, hexyldiketone, and tetrabutylammonium lithium phthalocyanine (TBA-LiPc) were carried out by literature procedures.[6] Coronene (sublimed, 99%) was obtained from Sigma-Aldrich and used as received.

2.2. Experimental Measurements. Hydrogen storage measurements were carried out using the equipment and calculations as previously described for the determination of the hydrogen adsorption of corannulene.[7] All materials were obtained as powders from purification procedures. The densities of all materials on which measurements were conducted were determined by standard techniques. The sample quantities were 3 g of each of the materials described above except for coronene (0.5 g). Li_2Pc and TBA-LiPc were dried at 160 °C under vacuum for 18 h prior to hydrogen storage measurements at Argonne. To ensure the validity of the H_2 uptake measurements, a carbon nanotube sample of known adsorption (provided by Penn State University) was used as a control. Hydrogen adsorption by the control carbon sample, as measured in our laboratory, was 0.67 wt % of H_2 adsorbed at 298 K and 72 bar. The control value as provided by Penn State was 0.7 wt % of H_2 adsorbed at 298 K and 75 bar. In addition, the densities of the aromatic materials as described in Tables 1, 2, and 3 were used to obtain the exact volume occupied by the sample inside of the holder and thus to calculate the adsorption appropriately.

2.3. Methods of Calculations. Ab initio calculations were conducted in this study to investigate the interaction of molecular hydrogen with an aromatic carbon adsorbent and with a negatively charged aromatic ring. Specifically, second-order Møller−Plesset (MP2) theory was used for all geometry optimizations for the reactants and products involved in the physisorption process. Geometries of neutral aromatic molecules were optimized by MP2 with all electrons included for electron correlation corrections using the 6-31G(d) basis set, MP2(Full)/6-31G(d). For geometry optimizations of phthalocyanine-type complexes such as dilithium phthalocyanine, frozen core MP2 (electrons of the inner shell were excluded in the calculation for correlation corrections) with the 3-21G basis set, MP2(FC)/3-21G, was employed. Vibrational frequency calculations with corresponding levels of MP2 theory showed that there were no imaginary frequencies for the reactants and products, thereby implying that each was at a local minimum. Thermal corrections obtained from the results of vibrational frequency calculations to the enthalpy or Gibbs energy for each reactant and product allow one to calculate the change in enthalpy or Gibbs energy for the physisorption process as a function of temperature, pressure, and the number of moles of molecular hydrogen used in the reaction. Thermochemistry analysis was conducted at the same temperatures and pressures as those used experimentally to determine the wt % of hydrogen stored based on the physisorption process. The thermal correction to enthalpy (TCEN) or Gibbs energy (TCGE) for the reaction, based on the difference of the individual values of the thermal correction terms for the products and reactants, when added to the binding energy of the adsorbent, yields the change in enthalpy or the change in Gibbs energy for the physisorption reaction. The magnitude of the thermal correction term is given by $\Delta E_{trans} + \Delta E_{rot} + \Delta E_{vib} + \Delta ZPE + \nu kT - T(\Delta S_{trans} + \Delta S_{rot} + \Delta S_{vib})$, where Δ corresponds to the difference between products and reactants and ν is the difference between the stoichiometric coefficients of products and reactants.[8] Each of the energy and entropy terms corresponds to the translational, rotational, and vibrational contributions of each molecule, and ZPE corresponds to the zero-point energy correction. This equation assumes that the contributions are additive. The thermal correction to Gibbs energy (TCGE) for the reaction is very useful since it defines what the binding energy of the adsorbent must be in order for a reaction to be thermodynamically allowed. The binding energies (BE) for all adsorbents were initially determined using either MP2(Full)/6-31G(d) or MP2(FC)/3-21G as a result of the geometry optimization. To be more accurate and representative of binding energies necessary for physisorption by an adsorbent, single-point calculations using MP2(Full)/6-311++G(3df,2p) were then carried out to determine the single-point binding energy (SPBE) of corannulene, isocorannulene, benzene, and bis(benzene) sandwich structures for use in calculating the change in enthalpy or Gibbs energy. All of the above calculations were carried out using Gaussian 03.[9] The GAMESS[10] package was also used in the calculation of the single-point energies (MP2(FC)/6-311++(3df,2p)) for coronene, the isocorannulene, and its derivatives, diketone and hexyldiketone.

Classical molecular dynamics (MD) simulations were used to introduce collective effects on a larger number of adsorbent molecules in contact with a gas phase consisting of H_2 molecules. Simulations were done in the NVT ensemble, that is, at a fixed number of molecules N, simulation cell volume V, and temperature T. Details of the MD simulations and the procedure to obtain the amount of H_2 adsorbed were provided in an earlier report.[7,22]

TABLE 1: Physisorption of *n* Hydrogen Molecules by Corannulene[a]

entry	adsorbent	*n*	*T*/*P*	SPBE	BE	TCEN	Δ*H*	TCGE	Δ*G*	wt % H_2 adsorbed	
										calc.	exp.
1	$C_{20}H_{10}$	1	298/73	−2.81	−0.94	+0.88	−1.93	+1.83	−0.98	0.79	0.93
2	$C_{20}H_{10}$	2	298/73	−3.61	−1.56	+1.88	−1.73	+4.18	+0.57	1.57	0.93
3	$C_{20}H_{10}$	2	77/45	−3.61	−1.56	+1.11	−2.50	+2.15	−1.46	1.57	1.50

[a] *T* (Kelvin), *P* (bar); SPBE, BE, TCEN, TCGE, Δ*H*, and Δ*G* expressed in kcal/mol. Geometry optimization and frequency calculations were done using MP2(Full)/6-31G(d).

TABLE 2: Physisorption of *n* Hydrogen Molecules Interacting with Isocorannulene, Diketone, and Hexyldiketone[a]

entry	adsorbent	*n*	*T*/*P*	SPBE	BE	TCEN	Δ*H*	TCGE	Δ*G*	wt % H_2 adsorbed	
										calc	exp
1	iso-$C_{20}H_{10}$	1	298/75	−2.18	−0.84	+0.91	−1.27	+1.56	−0.62	0.79	
2	iso-$C_{20}H_{10}$	1	77/45	−2.18	−0.84	+0.51	−1.67	+0.91	−1.27	0.79	
3	$C_{20}H_{10}O_2$	1	298/75	−1.52	−0.68	+0.94	−0.58	+1.77	+0.25	0.70	0.45
4	$C_{20}H_{10}O_2$	1	77/45	−1.52	−0.68	+0.54	−0.98	+0.99	−0.53	0.70	3.70
5	$C_{26}H_{22}O_2$	1	298/75	−1.65	−0.73	+0.93	−0.72	+1.94	+0.29	0.54	0.42
6	$C_{26}H_{22}O_2$	1	77/45	−1.65	−0.73	+0.54	−1.11	+1.03	−0.62	0.54	3.90

[a] *T* (Kelvin), *P* (bar); SPBE, BE, TCEN, TCGE, Δ*H*, and Δ*G* expressed in kcal/mol. Geometry optimization and frequency calculations were done using MP2(Full)/6-31G(d).

TABLE 3: Physisorption of *n* Hydrogen Molecules on Coronene[a]

entry	adsorbent	*n*	*T*/*P*	SPBE	BE	TCEN	Δ*H*	TCGE	Δ*G*	wt % H_2 adsorbed	
										calc	exp
1	$C_{24}H_{12}$	1	298/77	−1.51	−0.81	+0.92	−0.59	+1.51	0.00	0.66	0.75
2	$C_{24}H_{12}$	7	298/77	−7.74	−4.80	+6.77	−0.97	+14.65	+6.91	4.46	0.75
3	$C_{24}H_{12}$	7	77/45	−7.74	−4.80	+4.34	−3.40	+7.84	+0.10	4.46	4.60

[a] *T* (Kelvin), *P* (bar); SPBE, BE, TCEN, TCGE, Δ*H*, and Δ*G* expressed in kcal/mol. Geometry optimization and frequency calculations were done using MP2(Full)/6-31G(d).

3. Results and Discussion

3.1. Corannulene ($C_{20}H_{10}$). The calculated change in enthalpy and Gibbs energy for the physisorption process in which *n* hydrogen molecules are adsorbed onto the surface of corannulene at experimental temperatures and pressures is shown in Table 1. Calculations employing one hydrogen molecule on the concave surface of corannulene at 298 K and 73 bar (entry 1) give a 0.79 wt % absorption as compared to the experimental value of 0.93%. The calculated Δ*G* of −0.98 kcal/mol is consistent with the reaction being thermodynamically allowed. The calculated Δ*H* for this reaction is −1.93 kcal/mol and is a factor of 2 higher than the heat of adsorption associated with graphite (−0.9 kcal/mol)[11] and slightly higher than that for activated carbons, which ranges from −1.25 to −1.43 kcal/mol.[1,12] Okamoto has shown that the binding energy for molecular hydrogen can be increased by a factor of 3 by using curved graphene substrates as the adsorbent versus a planar graphene substrate.[13] In our prior investigation, the calculated binding energy for molecular hydrogen interacting with the concave surface was shown to be twice that of the convex surface.[7]

The experimental heats of adsorption for SWNT bundles and multiwall carbon nanotubes with open-ended structures are −4.84 and −3.94 kcal/mol, respectively.[14−16] These values are higher by at least a factor of 2 than the value calculated for corannulene interacting with one hydrogen molecule on the concave surface. If one takes into account that the adsorption sites associated with the experimental results may reflect increased multiwall molecular hydrogen interactions when compared to the concave surface of corannulene, higher enthalpies of adsorption are to be expected. Consistent with this, MD simulations[7] involving multiwall molecular hydrogen interactions, a "cooperative effect", show that the calculated hydrogen adsorption at 300 K and 40 bar is approximately 2 wt % when two corannulene molecules are separated by 8 Å. Experimentally, multiwall carbon nanotubes adsorb 1.97 wt % of H_2 at 300 K and 40 bar after being exposed to high-purity hydrogen for 5 h.[16] In view of the above discussion, the calculated Δ*H* of −1.93 kcal/mol appears to be reasonable.

The interaction of two hydrogen molecules with corannulene at 298 k and 73 bar (entry 2) is shown to be not thermodynamically allowed as Δ*G* is +0.57 kcal/mol. However, at 77 K and 45 bar, Δ*G* is −1.46 kcal/mol (entry 3), and the experimental 1.5 wt % of H_2 corresponds to two hydrogen molecules absorbed per corannulene molecule.

3.2. Isocorannulene ($C_{20}H_{10}$). The structures of isocorannulene and its derivatives diketone and hexyldiketone are shown in Figure 1. The diameter of the isocorannulene is approximately 7.13 Å as compared to the diameter of corannulene, which is approximately 6.47 Å, and therefore, one expects the isocorannulene binding energy to be lower because it is more planar. Table 2 shows the calculated binding energies for isocorannulene and its derivatives diketone and hexyldiketone interacting with one hydrogen molecule on the concave surface. The calculated binding energy of isocorannulene (entry 1) is −2.18 kcal/mol. This value is lower than that of corannluene, which is −2.81 kcal/mol, and is consistent with isocorannulene being more planar. The corresponding change in enthalpy of −1.27 kcal/mol is more in line with the experimental results for activated carbons. Entry 3 shows that the incorporation of two carbonyl groups in an isocorannulene-like molecule reduces the calculated binding energy to a value of −1.52 kcal/mol. The influence of electron-withdrawing groups in reducing binding energy is consistent[4,17] with a reduced hydrogen absorption value of 0.45 wt % when compared to corannulene at a similar temperature

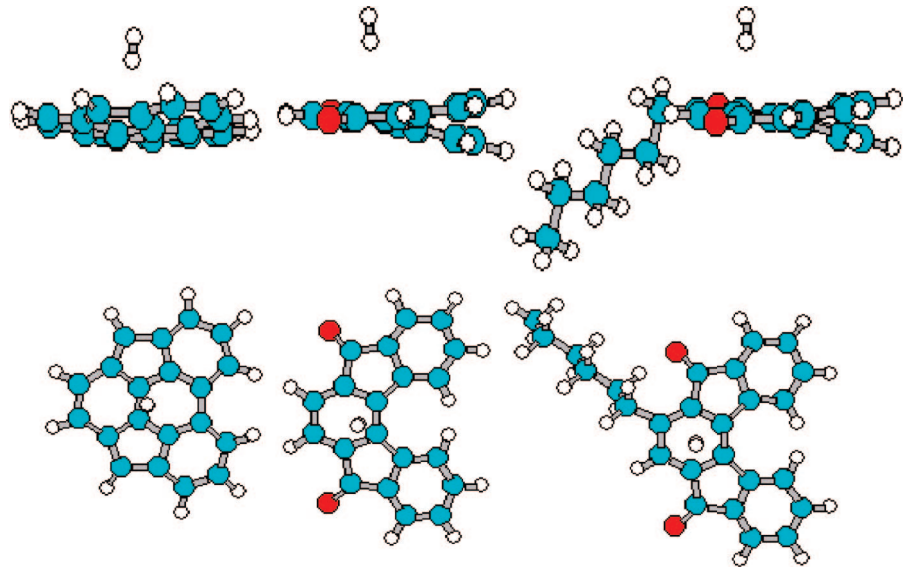

Figure 1. Geometry-optimized structures representing the adsorption sites for one hydrogen molecule interacting with isocorannulene (left), diketone (center), and hexyldiketone (right) using MP2(Full)/6-31G(d). The upper structures are side views, and the lower are top views (turquoise: carbon; red: oxygen).

TABLE 4: Calculated Binding Energy (BE) in kcal/mol for Phthalocyanine-Type Adsorbents Interacting with 14 H_2 Using MP2(FC)/3-21G for the Geometry Optimization of the Reactants and Product

entry	adsorbent	n	BE	BE/H_2	comments
1	[Li-Pc]$^-$	14	−21.54	−1.54	
2	Li_2Pc	14	−19.11	−1.37	
3	TMA-LiPc[a]	14	−19.44	−1.39	H_2 trans to TMA
4	TMA-LiPc[b]	13/1	−23.10	−1.65	13 H_2 cis to TMA; 1 H_2 trans to TMA

[a] Tetramethylammonium (TMA) lithium phthalocyanine with 14 H_2 molecules located on the side of the Pc ring opposite to the cation, TMA. [b] Tetramethylammonium (TMA) lithium phthalocyanine with 13 H_2 molecules located on the same side of the Pc ring as TMA and with 1 H_2 on the side opposite to TMA.

and pressure. Entry 3 shows that the calculated ΔG is slightly positive (+0.25 kcal/mol) for one hydrogen molecule ($n = 1$, 0.70 wt%) interacting with the diketone. Experimentally, 0.45 wt % of H_2 is adsorbed at 298 K and 75 bar, which corresponds to $n = 0.6$ adsorbed H_2 molecules.

Physisorption at 77 K (entry 4) shows that experimentally, approximately five hydrogen molecules are adsorbed (exp = 5 × calc). The effect of the addition of a C_6 alkyl group to the structure along with the carbonyl functional groups is to increase the binding energy to a value of −1.65 kcal/mol (entry 5). As in the previous case, ΔG is slightly positive, with a value of +0.29 kcal/mol for one hydrogen molecule interacting with the hexyldiketone at 298 K and 75 bar, but the calculated value of 0.54 wt % adsorbed is now more in line with the experimental value of 0.42 wt % adsorbed, corresponding to $n = 0.75$. At 77 K (entry 6), the number of hydrogen molecules experimentally observed interacting with the adsorbent is seven as compared to five interacting with the diketone. The consistency of these results in the context of the anticipated effects of reduced binding energy associated with planar molecules such as coronene versus corannulene and the addition of electron-withdrawing groups to a nearly planar derivative of corannulene seems to preclude packing or pore filling effects as significant factors in the experimental results. Even within the derivatives of corannulene, the effect of an alkyl substituent is realized since the number of hydrogen molecules adsorbed increases from 0.6 to 0.75, which can be obtained from the measured wt % H_2 values (entries 3 and 5, Table 2).

3.3. Coronene ($C_{12}H_{24}$). The calculated binding energy of molecular hydrogen interacting with the center ring of coronene is −1.51 kcal/mol (Table 3, entry 1) and is in good agreement with that reported by Hübner and Ferre-Vilaplana.[17,18] The calculated TCGE value is +1.51 kcal/mol and is consistent with both the calculated ΔG value of 0.0 kcal/mol and the corresponding experimental observation of one hydrogen molecule adsorbed, 0.75 wt %. The calculated change in enthalpy of −0.59 kcal/mol is in fairly good agreement with the value of −0.90 kcal/mol expected for graphite.[11] Entry 2 suggests that seven hydrogen molecules cannot be adsorbed at 298 K and 77 bar because the calculated ΔG is +6.91 kcal/mol. However, at a lower temperature of 77 K, it was experimentally observed that seven hydrogen molecules are adsorbed at 45 bar to give a value of 4.60 wt % (entry 3). The calculated ΔG, although slightly positive at +0.10 kcal/mol, could be viewed as a guide to the prospect for a physisorption process to be thermodynamically allowed.

The calculated and experimental results in Table 3 demonstrate how well the theoretical approach used in this investigation approximates the conditions required for a physisorption process to take place at a specified temperature and pressure when one considers that the SPBE and TCGE were determined independently.

3.4. Phthalocyanine Adsorbents (Li_2Pc, TMA-LiPc, TBA-LiPc). ***3.4.1. Binding Energy.*** In the context of achieving high hydrogen adsorption at or near ambient conditions, we have investigated the use of a negatively charged aromatic ring as a means to increase the binding energy of the adsorbent and will later consider the influence of a sandwich structure for lowering the binding energy requirement in order for the physisorption reaction to be thermodynamically allowed. The negatively charged aromatic ring used as an adsorbent in this investigation

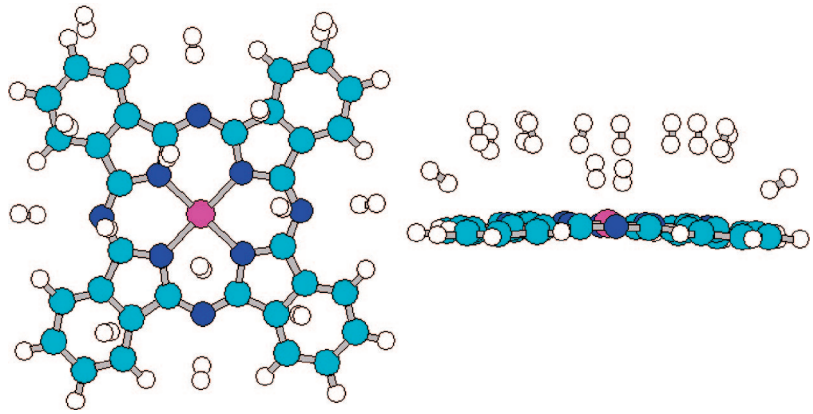

Figure 2. Calculated structure of complex anion, $[LiPc]^-$ interacting with 14 H_2 using MP2(FC)/3-21G for the geometry optimization (left: top view; right: edge view; turquoise: carbon; pink: lithium; blue: nitrogen).

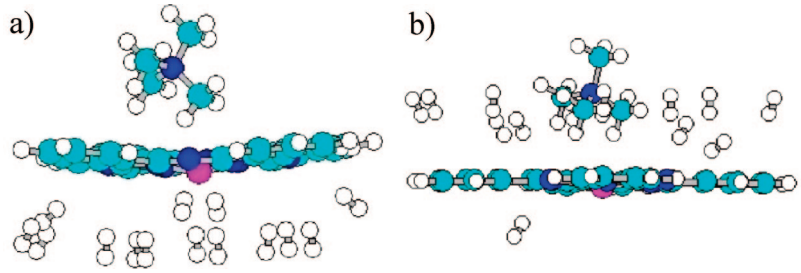

Figure 3. Calculated structures of TMA-LiPC interacting with 14 H_2 using MP2(FC)/3-21G for the geometry optimization with the TMA cation either trans (a) or cis (b) to H_2 (turquoise: carbon; pink: lithium; blue: nitrogen).

is the complex anion of dilithium phthalocyanine $[LiPc\ ]^-$. Figure 2 shows the interaction of 14 hydrogen molecules with the complex anion $[LiPc\ ]^-$.

There are four nonligand nitrogen atom sites for H_2 adsorption (the four outer nitrogen atoms not bonded with the lithium; Figure 2) where the separation distance between nitrogen and each of these hydrogen molecules is 2.52 Å. The average separation between the other 10 hydrogen molecules and the phthalocyanine ring is ~2.96 Å. The H−H bond length increase for the adsorbed hydrogen molecules is on the order of 0.002−0.004 Å when compared with the unbound H−H bond length of 0.741 Å, optimized using MP2(FC)/3-21G. The increase in the H−H bond length is consistent with that reported by Lochan and Head-Gordon for hydrogen interacting with the cyclopentadienyl anion, Cp^-,[4] where the anion causes a charge-induced dipole interaction illustrating an electrostatic interaction. For comparison, the Cp^- hydrogen molecule "end-on" separation distance is 2.53 Å, with a H−H bond length increase of 0.007 Å relative to the unbound H−H bond length. The greater increase of 0.007 Å may be due a greater localization of negative charge on Cp^- as compared with $[LiPc]^-$. The weakly perturbed H−H bond length for the interaction of hydrogen with $[LiPc]^-$ suggests that dispersion and electrostatic interactions are more important for the binding energy of the adsorbent than charge-transfer interactions, as discussed in ref 4.

Table 4 shows the calculated binding energy of various phthalocyanine-type adsorbents interacting with 14 H_2. The average binding energy associated with 14 H_2 interacting with $[LiPc]^-$ is −1.54 kcal/mol using MP2(FC)/3-21G for the geometry optimization of the reactants and product. Because it is calculated with the 3-21G basis set, the binding energy of −1.54 kcal/mol does not accurately reflect the binding energy for the adsorption process based on physisorption. As a first approximation, the calculated binding energy of −3.19 kcal/mol for one H_2 interacting with Cp^- using the cc-pVTZ basis set[4] is more in line with what one expects for the binding energy of the complex anion $[LiPc]^-$ interacting with one H_2.

Table 4, entry 2, shows that once the complex anion has been neutralized with another lithium ion, the binding energy per hydrogen molecule is −1.37 kcal/mol. This represents an 11% reduction in binding energy. Correspondingly, Lochan and Head-Gordon have found that once a lithium ion acting as a site for hydrogen adsorption is neutralized by a cyanide anion, the binding energy decreases by 52%.[4] The total binding energy of −19.11 kcal/mol (Table 4, entry 2) is approximately twice as great as that found for 14 hydrogen molecules interacting with corannulene on the convex side,[7] that is, −10.54 kcal/mol. This comparison suggests that an increase by a factor of 2 in binding energy is possible with a negatively charged aromatic molecule relative to a neutral aromatic molecule like corannulene.

The results shown in Table 4 for entries 3 and 4 also suggest that the phthalocyanine ring can accommodate hydrogen molecules on both sides of the phthalocyanine ring, including those adjacent to the tetramethylammonium cation (TMA). This is shown in Figure 3a and b. Experimental measurement of hydrogen adsorption using tetrabutylammonium lithium phthalocyanine (TBA-LiPc), to be discussed later, is consistent with hydrogen adsorption on both sides of the phthalocyanine ring.

3.4.2. Li_2Pc Adsorbent. The complex anion of Li_2Pc shows that the four nonligand nitrogen atoms are sites for hydrogen adsorption as well as other portions of the aromatic ring. In the case of Li_2Pc, the lithium ion is also an adsorption site for molecular hydrogen through an electrostatic charge−quadrupole interaction. This is illustrated in Figure 4, in which the separation between the lithium ion and hydrogen, as measured at the midpoint between hydrogen atoms, is 2.39 Å. As a comparison, on the basis of neutron powder diffraction studies, D_2 adsorption sites are located at a distance of 2.27 and 2.39 Å from Mn^{2+}(metal−organic framework) and Cu^{2+} [Cu_3(1,3,5-benzenetricarboxylate)$_2$], respectively.[19,20] The hydrogen binding, as

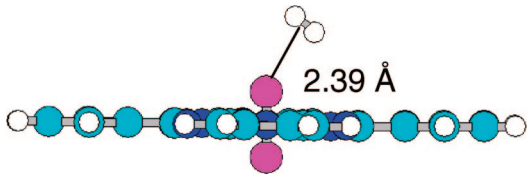

Figure 4. Optimized structure for Li_2Pc-H_2 interacting with a lithium ion using MP2(FC)/3-21G (turquoise: carbon; pink: lithium; blue: nitrogen).

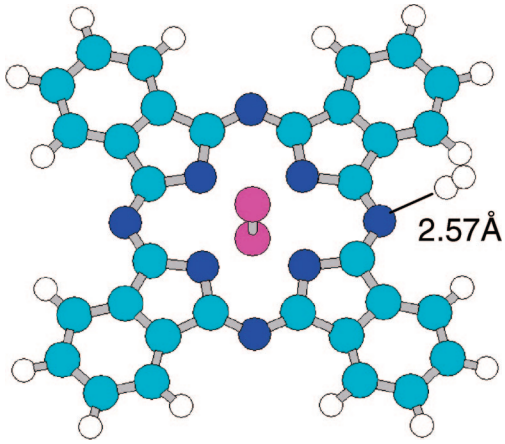

Figure 5. Optimized structure for Li_2Pc-H_2 interacting on a nonligand nitrogen atom using MP2(FC)/3-21G (turquoise: carbon; pink: lithium; blue: nitrogen).

shown in Figure 4, is through a side-on fashion, as discussed by Lochan and Head-Gordon.[4] The H−H separation distance is 0.746 Å and represents an increase of 0.005 Å versus the unbound hydrogen molecule, suggesting electrostatic interactions on the lithium ion site. The calculated binding energy based on MP2(FC)/3-21G for the geometry optimization of reactants and products is −2.14 kcal/mol. Correspondingly, the binding energy of one H_2 interacting with one of the four nonligand nitrogen atoms with an end-on fashion is −1.96 kcal/mol, with a separation distance of 2.57 Å. This is illustrated in Figure 5. Frequency calculations were carried out based on structures shown in Figures 4 and 5. In both cases, there were no imaginary frequencies, thereby illustrating that both structures were at a minimum on the potential energy surface. As discussed previously, ab initio calculations were accomplished at the same temperatures and pressures as those used for the experimental hydrogen adsorption measurements. The wt % of H_2 adsorbed experimentally at 298 K and 77 bar for Li_2Pc is 0.72 wt %. This value suggests that two H_2 are adsorbed per Li_2Pc. If the calculations were carried out for two hydrogen molecules interacting with Li_2Pc instead of one hydrogen, there should not be a dramatic reduction in binding energy due to repulsion. Lochan and Head-Gordon have shown that there is only about a 5% reduction in binding energy when two hydrogen molecules interact with a lithium cation through a charge−quadrupole type interaction.[4] Thus, as a first approximation, the thermodynamic quantities calculated using one hydrogen molecule should be appropriate.

Table 5 shows the calculated thermodynamic properties for the hydrogen adsorption site shown in Figure 4 where there is only one H_2 adsorbed. In order for the reaction to be thermodynamically allowed at 298 K and 77 bar, the TCGE value would suggest that a binding energy of −3.75 kcal/mol is required. Long et al.[19] have shown via neutron diffraction experiments that for a Mn^{2+} site within a metal−organic framework structure, the separation between the Mn^{2+} site and

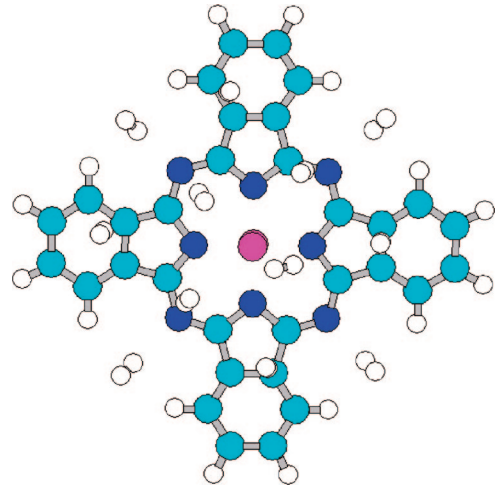

Figure 6. Optimized structure of $Li_2Pc-12H_2$ using MP2(FC)/3-21G (turquoise: carbon; pink: lithium; blue: nitrogen).

hydrogen is 2.27 Å, with a change in enthalpy at liquid nitrogen temperatures for this site equal to −2.41 kcal/mol and a pressure range of 0−1.2 bar. The calculated change in enthalpy for the lithium ion site shown in Figure 4 is −2.67 kcal/mol, assuming a binding energy of −3.75 kcal/mol. Due to the size of the phthalocyanine molecular system, calculations for the SPBE using the high-level basis set, 6-311++G(3df,2p), could not be accomplished, and therefore, a numeric value of 3.75 kcal/mol based on the calculated TCGE value is listed in Table 5 as an approximation of the binding energy.

Table 6 shows the calculated values of BE, TCEN, and TCGE for the nitrogen atom adsorption site as shown in Figure 5. Entry 1, Table 6 shows that TCGE is +4.62 kcal/mol for the nitrogen atom site, and correspondingly, a binding energy of −4.62 kcal/mol is required if the physisorption process is to be thermodynamically allowed at 298 K and 77 bar. The higher value of +4.62 kcal/mol versus a TCGE value of +3.75 kcal/mol (Table 5) suggests that perhaps only the lithium ion site is involved in hydrogen adsorption at 298 K and 77 bar. However, at 77 K and 45 bar (entry 2, Table 6), the total binding energy requirement of +21.23 kcal/mol (calculated for 12 hydrogen molecules interacting with Li_2Pc) is almost met by the binding energy calculated with the lower-level basis set of 3-21G with a value of −17.73 kcal/mol. Figure 6 shows that the predominant mode of H_2 interaction is through the aromatic phthalocyanine ring. These calculated results suggest that at 77 K/45 bar, the nitrogen atoms are the dominant adsorbent sites, which is consistent with the experimental result of 10 hydrogen molecules adsorbed, even though the calculations are based on 12 hydrogen molecules adsorbed.

A question that may not be readily apparent arises based on the investigation of Li_2Pc as an adsorbent. Do the experimental values associated with hydrogen adsorption indicate absorption on both sides of the phthalocyanine ring or just one side? Therefore, molecular dynamics simulations were used to model the adsorption of the test material Li_2Pc using χ-Li_2Pc as the adsorbent. X-ray diffraction analysis of single crystals of Li_2Pc show that the phthalocyanine ring separation is either 3.06 or 3.38 Å and, therefore, as in the case of graphite, would be too close to allow adsorption of hydrogen between the rings.[21] The separation between the layers of Li_2Pc molecules in χ-Li_2Pc used for the MD simulations is 3.4 Å.

Figure 7 shows the interaction of molecular hydrogen with χ-Li_2Pc and would suggest that no molecular hydrogen is adsorbed between the layers. MD simulations at 300 K and 77

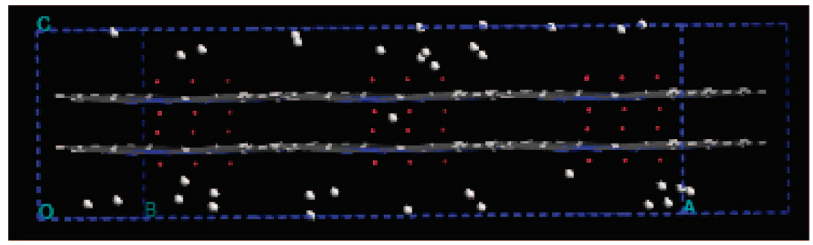

Figure 7. Snapshot from a MD simulation of hydrogen adsorption on χ-Li_2Pc adsorbed hydrogen.

TABLE 5: Physisorption of *n* Hydrogen Molecules on a Li_2Pc Lithium Adsorption Site As Shown in Figure 4[a]

entry	adsorbent	*n*	*T*/*P*	SPBE[b]	BE	TCEN	ΔH	TCGE	ΔG	wt % H_2 adsorbed	
										calc	exp
1	Li_2Pc	1	298/77	−3.75	−2.14	+1.08	−2.67	+3.75	0.00	0.38	0.72

[a] *T* (Kelvin), *P* (bar); SPBE, BE, TCEN, TCGE, ΔH and ΔG expressed in kcal/mol. Geometry optimization and frequency calculations done using MP2(FC)/3-21G. For $n = 1$, H_2 adsorption is at the lithium ion site. [b] Estimated value (see text).

TABLE 6: Physisorption of *n* Hydrogen Molecules on a Li_2Pc Nitrogen Adsorption Sites As Shown in Figures 5 and 6[a]

entry	adsorbent	*n*	*T*/*P*	BE	TCEN	TCGE	wt % H_2 adsorbed	
							calc	exp
1	Li_2Pc	1	298/77	−1.96	+1.34	+4.62	0.38	0.72
2	Li_2Pc	12	77/45	−17.73	+11.81	+21.23	4.36	3.80

[a] *T* (Kelvin), P (bar); BE, TCEN, and TCGE expressed in kcal/mol. Geometry optimization and frequency calculations done using MP2(FC)/3-21G. For $n = 1$, H_2 adsorption is at the nitrogen atom

TABLE 7: MD Simulation of Hydrogen Adsorption on χ-Li_2Pc

entry	temp (K)	pressure (bar)	H_2 uptake (wt %)	temp (K)	pressure (bar)	H_2 uptake (wt %)
1	273	201	1.97	300	201	1.66
2	273	136	1.40	300	136	1.19
3	273	97	1.07	300	102	0.94
4	273	76	0.84	300	77	0.71

TABLE 8: Physisorption of *n* Hydrogen Molecules on Benzene[a]

entry	adsorbent	*n*	*T*/*P*	SPBE	BE	TCEN	ΔH	TCGE	ΔG	calc wt % H_2 ads
1	C_6H_6	1	298/1	−1.19	−0.62	+0.94	−0.25	+4.16	+2.97	2.50
2	C_6H_6	1	298/50	−1.19	−0.62	+0.94	−0.25	+1.92	+0.73	2.50
3	C_6H_6	1	298/150	−1.19	−0.62	+0.94	−0.25	+1.29	+0.10	2.50
4	C_6H_6	1	298/200	−1.19	−0.62	+0.94	−0.25	+1.13	−0.06	2.50

[a] *T* (Kelvin), *P* (bar); SPBE, BE, TCEN, TCGE, ΔH, and ΔG expressed in kcal/mol.

bar were in excellent agreement with experimental results with a calculated value of 0.71 wt % of H_2 adsorbed (0.72 wt % of H_2, experimental) and is consistent with only two H_2 adsorbed per Li_2Pc. MD simulation results shown in Table 7 suggest that it is not until pressures of at least 136 and 201 bar that the third and fourth hydrogen molecules are adsorbed. Introduction of a tetrabutylammonium cation replacing a lithium ion (to be discussed below) shows that a third H_2 is adsorbed at 298 K and 75 bar and, in view of the discussion above, is on the Pc ring opposite to the other two adsorbed H_2.

3.4.3. Tetraalkylammonium Lithium Phthalocyanine Adsorbents. *3.4.3.1. Tetrabutylammonium Lithium Phthalocyanine (TBA-LiPc).* Molecular hydrogen adsorption was experimentally measured using tetrabutylammonium lithium phthalocyanine (TBA-LiPc). The wt % of H_2 adsorbed for TBA-LiPc at 298 K and 75 bar is 0.72 wt % and corresponds to three hydrogen molecules adsorbed. As discussed above for χ-Li_2Pc, the third hydrogen molecule is not expected to be adsorbed until a pressure of 136 bar. Therefore, in the case of TBA-LiPc at 298 K and 75 bar, it is quite likely that the third hydrogen is added to the other side of the ring not occupied by the first two hydrogen molecules. At 77 K and 45 bar, the wt % H_2 adsorbed for TBA-LiPc is 5.93 wt %. This corresponds to 24 hydrogen molecules adsorbed per TBA-LiPC and strongly supports that both sides of the negatively charged phthalocyanine ring are involved in hydrogen adsorption. These results suggest that the replacement of one lithium ion with the TBA cation disrupts the close proximity of the phthalocyanine rings as in the case of Li_2Pc and makes available both sides of the phthalocyanine ring for hydrogen adsorption.

3.4.3.2. MD Simulations of Tetramethylammonium Lithium Phthalocyanine (TMA-LiPc). Molecular dynamics simulations were used to investigate the adsorption of molecular hydrogen with a layered molecular system of TMA-LiPc. Density functional theory was used to determine some of the force field parameters for the TMA-LiPc/H_2 interactions, which were represented by a Lennard-Jones potential including dipole-induced dipole interactions. Full details of the force field development are given in a separate publication.[22] MD simulations were performed on a periodic system with a unit cell

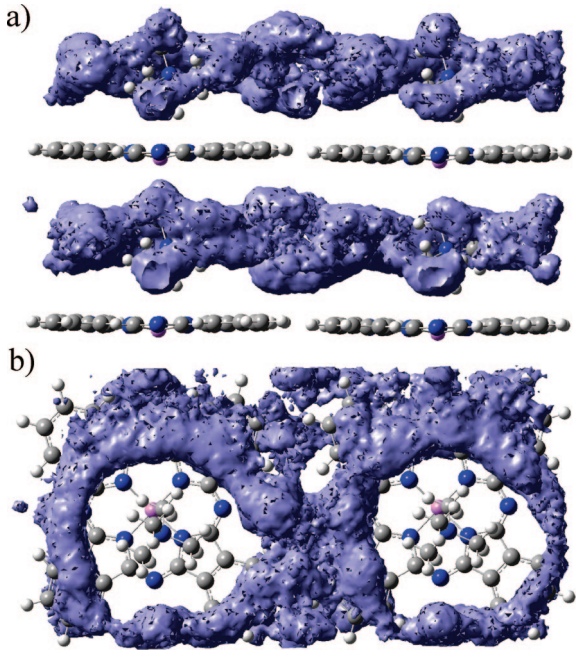

Figure 8. TMA-LiPc H_2 probability surface at constant temperature (300 K), approximately constant pressure (43 bar), and an ILD of 8.49 Å. The illustrations above are (a) side view and (b) end view.

containing 18 molecules of TMA-LiPc in a 3 × 3 × 2 stacked cubic arrangement with 770 H_2 molecules. The system volume was adjusted to match the desired initial pressure. Each simulation produced a single isotherm point on the pressure uptake graph representing an average of 251 snapshots.

The TMA-LiPc molecules were frozen, and only Lennard-Jones interactions were allowed between them and the H_2 molecules and between pairs of H_2 molecules. Since the crystalline structure of TMA-LiPc is not known, we have assumed that these materials may nucleate in layered structures. DFT calculations in dimers were utilized to obtain an estimate of the interlayer distance (ILD), and MD simulations were then run on TMA-LiPc layered structures to estimate H_2 adsorption isotherms at 77, 177, 236, 273, and 300 K.

Each simulation ran for a total of 800 ps, with the first 300 ps used to reach equilibrium and the remaining 500 ps recording system configurations every 2 ps, for a total of 251 system configurations. For each system configuration, the percent weight uptake of H_2 in the crystal was calculated, and the number of H_2 molecules in the gas phase was counted. All H_2 molecules not located within the gas-phase region were assumed to be adsorbed. The pressure in the gas-phase region was approximated by the ideal gas law. The weight uptake is the ratio of the mass of H_2 adsorbed over the mass of crystal plus the mass of H_2 adsorbed.

Figure 8 shows the H_2 probability surface between two layers of TMA-LiPc separated by 8.49 Å. One can note that the hydrogen molecules appear to be repulsed to the outer edges of the phthalocyanine ring by the TMA cation. This was also observed in ab initio calculations (see Figure 3a and b). Figure 8 also suggests that both sides of the phthalocyanine ring are acting as sites for hydrogen adsorption.

The effect of a layered molecular system of TMA-LiPc, as shown in Figure 8, is that approximately twice the amount of hydrogen is adsorbed when compared with the experimental value associated with TBA-LiPc. The calculated adsorption isotherms for H_2 in a hypothetical stacked structure of TMA-LiPc at different interlayer distances were reported elsewhere.[22] For example, the MD simulations predict a value of 1.25 wt % of H_2 adsorbed at 300 K and 75 bar with a separation of 10 Å. This represents an increase of 74% when compared with the monolayer of TMA-LiPc. In a separate set of calculations, the wt % of H_2 adsorbed for a monolayer of TMA-LiPc at 300 K and 75 bar is 0.72 wt %.[22] By taking into account differences of molecular weight between TMA-LiPc and TBA-LiPc, one would predict an experimental value of 0.92 wt % of H_2 adsorbed for a monolayer of TMA-LiPc at 298 K and 75 bar. The predicted experimental value of 0.92 wt% H_2 is slightly higher than 0.72 wt %, but without further structural characterization, one cannot completely confirm that TBA-LiPc is functioning only as a monolayer. These results are consistent with the importance of the negatively charged phthalocyanine ring as the active site for hydrogen adsorption.

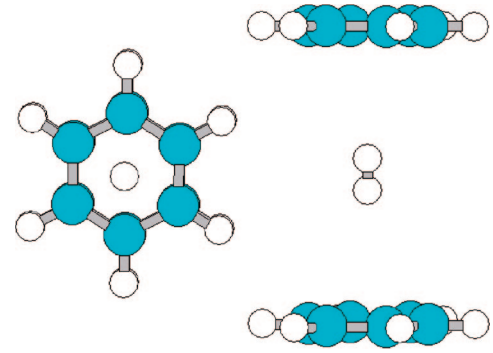

Figure 9. Optimized structure of bis(C_6H_6)−H_2 using MP2(Full)/6-31G(d) (turquoise: carbon).

As discussed above, layered molecular systems are important for increasing or doubling the binding energy of an adsorbent for H_2 adsorption. The next section will discuss the effectiveness of sandwich or layered structures in increasing the binding energy of the adsorbent and in reducing the binding energy requirements in order for a physisorption process to be thermodynamically allowed.

3.5. Sandwich Structures. ***3.5.1. Bis(corannulene)−5H₂ (Bis($C_{20}H_{10}$)−5H₂).*** In our previous investigation, it was shown that sandwich structures in which the interaction of molecular hydrogen is with the concave and convex surfaces of adjacent corannulene molecules could result in a doubling of the binding energy with molecular hydrogen (see Figure 8 and Table 2, entry 9, of ref 7). In the current investigation, the frequency calculation was completed for bis($C_{20}H_{10}$)−$5H_2$. The TCGE value is +39.84 kcal/mol at 298 K and 1 bar. Because of the size of the bis($C_{20}H_{10}$)−5H molecular system, MP2(FC)/3-21G was used for both the geometry optimization and frequency calculations instead of MP2(Full)/6-31G(d) as used in ref 7 for $C_{20}H_{10}$−$5H_2$-cvx (convex) and $C_{20}H_{10}$−$5H_2$-cc (concave). It has been found when investigating the interaction of molecular hydrogen with corannulene, whether using MP2(FC)/3-21G or MP2(Full)/6-31G(d), that similar TCGE values are obtained. For example, the interaction of molecular hydrogen on the convex surface of corannulene using MP2(FC)/3-21G has a TCGE value of +4.33 kcal/mol at 298 K and 1 bar. If one uses MP2(Full)/6-31G(d) to describe this interaction, the TCGE value is +4.31 kcal/mol at 298 K and 1 bar. On the basis of calculated TCGE values for $C_{20}H_{10}$−$5H_2$-cvx (convex) and $C_{20}H_{10}$−$5H_2$-cc (concave), a total additive TCGE value of +47.97 kcal/mol at 298 K and 1 bar is obtained. Since the TCGE value for the sandwich structure is +39.84 kcal/mol, the implication of these calculations suggests that layered or sandwich structures could result

TABLE 9: Physisorption of *n* Hydrogen Molecules in Sandwich Structure Bis(C_6H_6)[a]

entry	adsorbent	*n*	*T*/*P*	SPBE	BE	TCEN	Δ*H*	TCGE	Δ*G*	Calc wt % H_2 ads
1	bis-C_6H_6	1	298/1	−2.63	−1.11	+2.11	−0.52	+6.50	+3.87	1.27
2	bis-C_6H_6	1	298/50	−2.63	−1.11	+2.11	−0.52	+2.03	−0.60	1.27
3	bis-C_6H_6	1	298/100	−2.63	−1.11	+2.11	−0.52	+1.24	−1.39	1.27
4	bis-C_6H_6	1	298/150	−2.63	−1.11	+2.11	−0.52	+0.78	−1.85	1.27
5	bis-C_6H_6	1	298/200	−2.63	−1.11	+2.11	−0.52	+0.45	−2.18	1.27

[a] *T* (Kelvin), *P* (bar); SPBE, BE, TCEN, TCGE, Δ*H*, and Δ*G* expressed in kcal/mol.

in lowering the binding energy requirement in order for a physisorption process to be thermodynamically allowed.

3.5.2. Bis(C_6H_6)−H_2. A sandwich structure involving the use of benzene was investigated to further test the beneficial results described above. Initially, the binding energy of benzene with molecular hydrogen was evaluated using MP2(Full)/6-31G(d) for both the geometry and frequency calculations. Single-point calculations for determining the binding energy with molecular hydrogen were run using MP2(Full)/6-311++G(3df,2p). Table 8 shows the calculated results for molecular hydrogen interacting with benzene. The single-point binding energy of −1.19 kcal/mol is very similar to that reported in refs 17 and 18. Table 9 shows similar calculated results for the bis(C_6H_6) sandwich structure, and Figure 9 illustrates the interaction of the sandwich structure with molecular hydrogen. The average separation between benzene rings is 6.75 Å, and the hydrogen molecule is located within either 2.98 or 3.03 Å of the center of the benzene ring. The H−H bond length is 0.739 Å, which is an increase of 0.001 Å over the unbound H−H distance based on MP2(Full)/6-31G(d) calculation. All calculations for the bis(C_6H_6) sandwich structure were identical to those obtained in the benzene case. The benefit of the sandwich structure illustrates that the physisorption process may now be thermodynamically allowed at 50 bar versus 150 or 200 bar for benzene.

4. Conclusions

A range of structures having curved, planar, neutral, and charged characteristics have been evaluated both experimentally and theoretically. Charged systems (anionic) include electrostatic forces in addition to van der Waals forces, resulting in binding energies double the magnitude that of neutral aromatic molecules such as coronene. Layered anionic structural advantages include a total binding energy of approximately a factor of 4 larger than neutral aromatic molecules and include the possible benefit that the binding energy requirement for a physisorption process to be thermodynamically allowed may be reduced as expressed through a lower operating pressure.

Acknowledgment. The authors would like to acknowledge hydrogen storage determinations done at Argonne National Laboratory, Office of Basic Energy Sciences, Division of Chemical Sciences, Geosciences, and Biosciences, under DOE Contract DE-AC02-06CH11357. Computing resource were provided by the Air Force Research Laboratory, Major Shared Resource Center of DOD High Performance Computing Modernization Program.

References and Notes

(1) Bhatia, S. K.; Myers, A. L. Optimum conditions for adsorptive storage. *Langmuir* **2006**, *22*, 1688–1700.

(2) Benard, P.; Chahine, R. Determination of the adsorption isotherms of hydrogen on activated carbons above the critical temperature of the adsorbate over wide temperature and pressure ranges. *Langmuir* **2001**, *17*, 1950–1955.

(3) Züttel, A. Materials for hydrogen storage. *Mater. Today* **2003**, 24–33.

(4) Lochan, R. C.; Head-Gordon, M. Computational studies of molecular hydrogen binding affinities: The role of dispersion forces, electrostatics, and orbital interactions. *Phys. Chem. Chem. Phys.* **2006**, *8*, 1357–1370.

(5) Zhao, Y.; Kim, Y-H.; Dillon, A. C.; Heben, M. J.; Zhang, S. B. Hydrogen storage in novel organometallic buckyballs. *Phys. Rev. Lett.* **2005**, *94*, 155504/1–155504/4.

(6) (a) Corannulene was provided by James Mack. (b) Underwood, K. Hydrogen Storage and the Synthesis of 5,8-Dihydroindeno[2,1-c]fluorenes. M.Sc. Thesis, Wright State University, Dayton, OH, 2006,(c) Homborg, H.; Kalz, W. Preparation and characterization of tetraalkylammonium lithium phthalocyanines. *Z. Naturforsch., B: Anorg. Chem. Org. Chem.* **1978**, *33B*, 968–975.

(7) Scanlon, L. G.; Balbuena, P. B.; Zhang, Y.; Sandi, G.; Back, C. K.; Feld, W. A.; Mack, J.; Rottmayer, M. A.; Riepenhoff, J. L. Investigation of corannulene for molecular hydrogen storage via computational chemistry and experimentation. *J. Phys. Chem. B* **2006**, *110*, 7688–7694.

(8) Foresman, J. B, Frisch, Æ. *Exploring Chemistry with Electronic Structure Methods*, 2nd ed.; Gaussian, Inc.: Pittsburgh, Pa.

(9) Frisch, M. J.; Trucks, G. W.; Schlegel, H. B.; Scuseria, G. E.; Robb, M. A.; Cheeseman, J. R.; Montgomery, J. A., Jr.; Vreven, T.; Kudin, K. N.; Burant, J. C.; Millam, J. M.; Iyengar, S. S.; Tomasi, J.; Barone, V.; Mennucci, B.; Cossi, M.; Scalmani, G.; Rega, N.; Petersson, G. A.; Nakatsuji, H.; Hada, M.; Ehara, M.; Toyota, K.; Fukuda, R.; Hasegawa, J.; Ishida, M.; Nakajima, T.; Honda, Y.; Kitao, O.; Nakai, H.; Klene, M.; Li, X.; Knox, J. E.; Hratchian, H. P.; Cross, J. B.; Bakken, V.; Adamo, C.; Jaramillo, J.; Gomperts, R.; Stratmann, R. E.; Yazyev, O.; Austin, A. J.; Cammi, R.; Pomelli, C.; Ochterski, J. W.; Ayala, P. Y.; Morokuma, K.; Voth, G. A.; Salvador, P.; Dannenberg, J. J.; Zakrzewski, V. G.; Dapprich, S.; Daniels, A. D.; Strain, M. C.; Farkas, O.; Malick, D. K.; Rabuck, A. D.; Raghavachari, K.; Foresman, J. B.; Ortiz, J. V.; Cui, Q.; Baboul, A. G.; Clifford, S.; Cioslowski, J.; Stefanov, B. B.; Liu, G.; Liashenko, A.; Piskorz, P.; Komaromi, I.; Martin, R. L.; Fox, D. J.; Keith, T.; Al-Laham, M. A.; Peng, C. Y.; Nanayakkara, A.; Challacombe, M.; Gill, P. M. W.; Johnson, B.; Chen, W.; Wong, M. W.; Gonzalez, C.; Pople, J. A. *Gaussian 03*, revision A.7; Gaussian, Inc.: Pittsburgh, PA, 2004.

(10) GAMESS, 24MAR07 [R1], see: Schmidt, M. W.; Baldridge, K. K.; Boatz, J. A.; Elbert, S. T.; Gordon, M. S.; Jensen, J. H.; Koseki, S.; Matsunaga, N.; Nguyen, K. A.; Su, S. J.; Windus, L.; Montgomery, J. A. *J. Comput. Chem* **1993**, *14*, 1347.

(11) Dericbourg, J. Adsorption of hydrogen on the surface of graphite. *Surf. Sci.* **1976**, *59*, 565–574.

(12) Cheng, H.; Cooper, A. C.; Pez, G. P.; Kostov, M. K.; Piotrowski, P.; Stuart, S. J. Molecular dynamics simulations on the effects of diameter and chirality on hydrogen adsorption in single walled carbon nanotubes. *J. Phys. Chem. B* **2005**, *109*, 3780–3786.

(13) Okamoto, Y.; Miyamoto, Y. Ab initio investigation of physisorption of molecular hydrogen on planar and curved graphenes. *J. Phys. Chem. B* **2001**, *105*, 3470–3474.

(14) Shiraishi, M.; Takenobu, T.; Yamada, A.; Ata, M.; Kataura, H. Hydrogen storage in single-walled carbon nanotube bundles and peapods. *Chem. Phys. Lett.* **2002**, *358*, 213–218.

(15) Shiraishi, M.; Takenobu, T.; Ata, M. Gas-solid interactions in the hydrogen/single-walled carbon nanotube system. *Chem. Phys. Lett.* **2003**, *367*, 633–636.

(16) Lee, H.; Kang, Y. S.; Kim, S. H.; Lee, J. Y. Hydrogen desorption properties of multiwall carbon nanoyubes with closed and open structures. *Appl. Phys. Lett.* **2002**, *80*, 577–579.

(17) Hübner, O.; Glöss, A.; Fichtner, M.; Klopper, W. On the interaction of dihydrogen with aromatic systems. *J. Phys. Chem. A* **2004**, *108*, 3019–3023.

(18) Ferre-Vilaplana, A. Nunerical treatment discussion and *ab initio* computational reinvestigation of physisorption of molecular hydrogen on graphene. *J. Chem. Phys.* **2005**, *122*, 1047091−104709−10.

(19) Dincă, M.; Dailly, A.; Liu, Y.; Brown, C. M.; Neumann, D. A.; Long, J. R. Hydrogen storage in a microporous metal-organic framework with exposed Mn^{2+} coordination sites. *J. Am. Chem. Soc.* **2006**, *128*, 16876–16883.

(20) Peterson, V. K.; Liu, Y.; Brown, C. M.; Kepert, C. J. Neutron powder diffraction study of D_2 sorption in Cu_3(1,3,5-benzenetricarboxylate)$_2$. *J. Am. Chem. Soc.* **2006**, *128*, 15578–15579.

(21) Grossie, D. A.; Feld, W. A.; Scanlon, L.; Sandi, G.; Wawrzak, Z. Di-μ-acetone-κ^2O:O-bis[(acetone-κO)aqualithium(I)] di-μ-acetone-κ^2O:O-bis [(diaqualithium(I)] tetrakis{[phthalocyaninato(2-)- κ^4N,N′,N″,N‴] lithiate(I)}. *Acta Crystallogr.* **2006**, *E62*, m827–m829.

(22) Lamonte, K.; Gomez-Gualdron, D. A.; Scanlon, L. G.; Sandi, G.; Feld, W.; Balbuena, P. B. Molecular dynamics simulations of hydrogen adsorption in tetramethyl ammonium lithium phthalocyanine crystalline structures. *J. Phys. Chem. B* **2008**, *112*, 15775–15782.

JP809097V